KAI BERGER
berger@cg.tu-bs.de
Computer Graphics Lab, TU Braunschweig

IVO IHRKE
ihrke@mpi-sb.mpg.de
MMCI, Saarbrücken

Prof. Dr. Ing. MARCUS MAGNOR
magnor@cg.tu-bs.de
Computer Graphics Lab, TU Braunschweig

Refractive Index Dependent Bidirectional Scattering Distribution Functions

Technical Report 2010-11-0

November 30, 2010

Computer Graphics Lab, TU Braunschweig

Contents

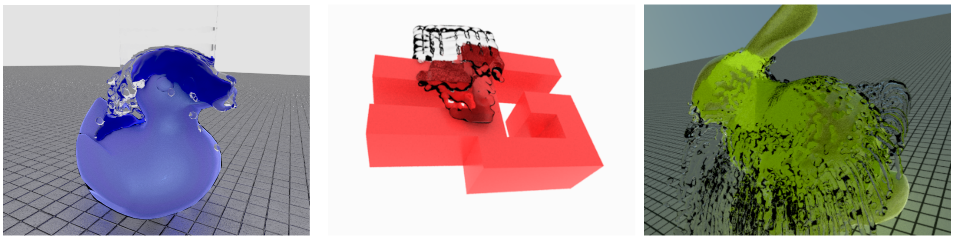

Figure 1: The interaction with media that have different refractive indices causes differences in the reflectance behaviors of surfaces. In this paper we capture BRDF data of materials showing this behavior and we fit a new model to enable rendering of such immersed materials. The left image shows a duck spilled with distilled water (refractive index 1.33). The material is blue cloth from our captured BRDF database. The middle image shows the Eurographics logo spilled with a salt solution (refractive index 1.44). The material is plastic synthesized by the proposed model. The right image shows the Stanford bunny spilled with distilled water. The material is bamboo synthesized by the proposed model. Notice how the brightness of the reflected light and the shape of the highlights changes.

Abstract

We investigate the effect of immersing real-world materials into media of different refractive indices. In theory, the reflective and transmissive behavior of a material that is immersed into surrounding media with different refractive indices should be predicted by the Fresnel equations. However, as we show, only a subclass of materials follows this theoretical model. In reality, many materials exhibit unexpected effects such as stronger localized highlights or a significant increase in the glossy reflection due to microgeometry. In our experiments we found that the variation of these effects can be quite strong, and none of the existing BRDF models realistically reproduce these effects seen in reality. We propose a new, parametric model that takes refractive index changes into account. We fit measurements of different materials and present results to demonstrate the importance of BRDF changes for submerged objects.

1 Introduction

A familiar effect in everyday life is that objects change their appearance when immersed in water or other substances with refractive indices different from air, Fig. 1. Some common examples include diffusers that lose their diffusing characteristics when coated e.g. with oil, becoming more transparent in the process. Another effect is the subtly different appearance of objects underwater that are observed, e.g., during diving: Picking up an object observed under water and observing it on the beach when dry will usually result in quite a different look.

This *refractive index dependence* of bidirectional scattering distribution functions (BSDFs) has so far been mostly ignored. Implicitly it is assumed to be governed by the Fresnel equations via the refractive index dependence of the Fresnel reflection and transmission factors, as are used in most physics-based BRDF models [TS67, CT81, HTSG91, APS00]. An exception is the BRDF model for finished wood by Marschner et al. [MWAM05]. Here, however, the focus is on the refractive properties of the surface finishing. The surrounding medium is still assumed to be air.

In this paper we measure the reflectance properties of a range of materials in the presence of a refractive immersing medium such as water or salt solutions. We analyze the acquired data to determine the applicability of current BRDF models to render underwater objects or objects otherwise immersed in refractive media (such as surface inclusions in glass).

We analyze the dependence of current physics-based BRDF models on the refractive index of the immersing medium. In particular, we show that the Fresnel term is the governing factor in those models. We proceed by theoretically analyzing the behavior of the Fresnel equations when changing the refractive index of the incident medium. We present a measurement apparatus to measure BSDFs in different refractive media and acquire a database of a wide range of representative materials. We verify the predictions made by our theoretical analysis on these real-world samples.

The paper is structured as follows: After revisiting the related work in the field of BRDF capturing and modeling in Section 2, we give a short overview about specular reflection and refraction at material boundaries in Section 3. We show that the Fresnel term is the governing factor for the surface appearance of materials placed into different media. We then introduce our measurement setup in Section 4 and the fitting of our enhanced BRDF model in Section 5. We validate the model and present the result in Section 6 before we conclude in Section 7.

2 Related Work

Phenomological Models are based on an intuitive modeling of the reflection process such as the famous Phong model [Pho75]. Usually, purely ad-hoc methods such as the original Phong model, and *physically plausible* BRDF models fall into this category where the latter characterization refers to the fact that ad-hoc models can be built such that they do not obviously violate the principles of positivity, reciprocity, and energy conservation. Examples include the generalized Phong model of Lafortune et al. [LFTG97], approximations of physical models as in Schlick [Sch94], the reflection model for metallic surfaces by Kelemen and Szirmay-Kalos [KSK01], or the approximation of subsurface scattering processes by Jensen et al. [JMLH01].

Physics-Based Models originated in the optics literature. The seminal work of Torrance and Sparrow [TS67] was introduced to computer graphics by Blinn [Bli77]. Cook and Torrance [CT81] extended the micro-facet model to use Beckmann's [BS63] micro-facet distribution function. Kajiya [Kaj85] developed a micro-faced model for anisotropic rough surfaces, based on an integral description using wave optics. He tabulated the BRDF values for efficient computation. A physics-based analytical model for anisotropic reflection was introduced by Poulin and Fournier [PF90]. A model based on physical optics, i.e. on electro-magnetic theory, was developed by He et al. [HTSG91]. All previously discussed models assume perfectly Fresnel reflecting micro-facets as a basis for the analytical derivation of the model. In addition, a regular micro-surface geometry like v-grooves is assumed to compute the geometry term. Oren and Nayar [ON94] instead consider micro-geometry consisting of perfect Lambertian reflectors while retaining the regular micro-geometry assumption. They show that a rough surface consisting of such facets has appreciable non-Lambertian reflectance. Ashikmin et al. [APS00] remove the regular micro-geometry assumption, developing a method to compute a suitable micro-geometry for a given, even designed, BRDF. Physics-based models inherently ensure BRDF energy conservation, reciprocity, and positivity properties of the resulting function.

Measurement-Based Models take a different approach. Instead of creating models from analytical descriptions of physical processes, they are based on measurements of the reflection properties of real-world materials. Suitable functions that describe the observed behavior are then fitted while preserving the basic BRDF properties as in the phenomenological models. Examples of this approach are the anisotropic Ward model [War92]. He et al. [HTSG91] also show fits of their physics-based model to real-world data. The Lafortune model [LFTG97] was specifically developed to fit observed data well. A different approach is taken by Matusik et al. [MPBM03a]. The authors acquire a large data base of reflectance data for a wide range of materials. They then analyze the data using PCA and nonlinear dimensionality reduction techniques [Bra03] to derive a low-parametric model given the initial data. Kautz et al. [KM99] present a method that uses spherical harmonics as representation for the captured data.

BRDF Acquisition has been performed using a variety of devices. The most commonly used tool in optics is the gonioreflectometer, where a planar sample is analyzed by a hemispherical adjustable detector and light source. Marschner et al. [MWLT00] developed an image-based BRDF measurement technique based on spherical samples. This way, moving the detector can be avoided and BRDFs with a high resolution in the viewing direction can be acquired. This technique is the prevailing technique for BRDF acquisition in graphics. Matusik et al. [MPBM03c] use a similar setup but propose to reduce the number of measurements by using their data base [MPBM03a]. An evaluation of analytical BRDF models for data fitting purposes has been performed by Ngan et al. [NDM05]. Ghosh et al. [GHAO08] expand the BRDF measurements in an optical basis and directly measure the basis coefficients, removing the need for any mechanical parts. Recently, Hullin et al. [HHA+10] have extended the concept of a monochromatic BRDF to account for bi-spectral interaction, i.e. conversion of the wavelength of light by the material as e.g. in fluorescent materials. They do not develop a model based on their measured data.

Methods for acquiring spatially varying BRDFs have also been developed [Dan01, LKG+03, MMS+05] but are of less interest in the context of the proposed method.

BTDF

The bidirectional transmittance distribution function (BTDF) models describe the transmission of light at the boundary of materials. While Dai et al.[DWL+09] and Walter et al. [WMLT07] present BTDF models for the entire entrance and exit process of light, the following papers present BTDFs for subsurface effects of opaque materials. Weidlich et al. [WW07] describe a multi-layer model for rendering of metallic paints or frosted metal and Hanrahan et al. [HK93] describe a layered surface model for subsurface reflectance that takes the Fresnel effect into account. The interaction of water with surfaces has been adressed by some papers beforehand. Lu et al. [LGR+05] describe the geometry-based drying process of objects spilled with water and Sun et al. [SSR+07] describe time-varying BRDFS (TV-BRDFs), for example dust accumulation and the drying of spray and oil paint. Gu et al. [GRBN07] describe a thin-layer BTDF model for rendering dirty and contaminated glass.

All previously presented methods do not account for intensity changes of reflected light for submerged surfaces. Our work addresses this gap and presents a suitable microfacet-based BRDF model and a method to measure data for materials whose reflectance behavior is governed by this effect.

3 Background

Specular reflection and refraction at material boundaries is caused by a change of the electric and magnetic fields across the interface. The exact description of the effect requires electromagnetic wave optics, i.e., solutions must satisfy Maxwell's equations. In graphics, however, geometric optics is the dominant model for describing and simulating the effects of light's interaction with matter. The basic tool for describing general reflections in graphics is the bidirectional reflectance distribution function (BRDF), and similarly, the bidirectional transmittance distribution function (BTDF) for refracted rays. Together these two functions are known as bidirectional scattering distribution function (BSDF). The BSDF can be considered the mean reflectance and transmittance of a material due to micro-scale global illumination effects at material structures much smaller than the incident beam spot size.

Physics-based BRDF models, which are often used to also describe BTDF's[WMLT08], are based on analytical derivations which are usually based on a specific surface micro-geometry and reflection model. Most commonly, perfectly mirroring micro-facets, so called Fresnel reflectors, are assumed as the basic building blocks of the micro-geometry [TS67, CT81, HTSG91, APS00, MWAM05].

Fresnel Reflection and Transmission are the main factors in these models that influence non-diffuse surface appearance. They are generally of the form [HTSG91]:

$$f_r = \lambda_s \rho_s + \lambda_{dd} \rho_{dd} + \lambda_{ud} \rho_{ud}, \tag{1}$$

where λ_s, λ_{dd} and λ_{ud} are the color multiplicative factors and ρ_s denotes perfect specular reflectance, ρ_{dd} directionally diffuse reflectance, ρ_{ud} perfect Lambertian reflectance, and f_r is the resulting BRDF. The specular and directionally diffuse terms are influenced by Fresnel reflection which enters the equation as a multiplicative factor

$$\rho_s = F_r \cdot L_i \tag{2}$$
$$\rho_{dd} = F_r \cdot D \cdot S, \tag{3}$$

where L_i is the incident radiance, D is the statistical micro-facet distribution, S is the shadowing term, and F_r is the Fresnel reflection coefficient. In the following, we assume unpolarized light as this is the most common

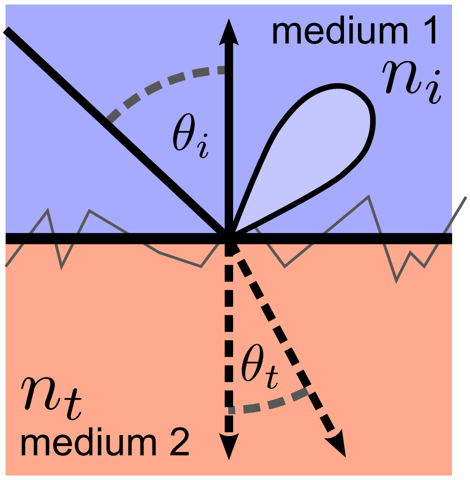

Figure 2: Geometry for micro-facet BRDF models. An incident ray makes an angle θ_i with the surface normal. The surface is assumed to be a flat interface, representing the mean of the surface micro-geometry (grey). The interface is separating two media with refractive indices n_i and n_t, respectively. Observe that opaque materials also have refractive indices, e.g. plastic has an index of ≈ 1.46. The Fresnel equations determine the amount of reflected and transmitted light. The lobe of the BRDF is indicated in light blue.

situation in computer graphics. The Fresnel reflection coefficient F_r is then given by

$$F_r = \frac{1}{2}\left(r_\perp^2 + r_\parallel^2\right) \tag{4}$$

$$r_\perp = \frac{(n_i \cos\theta_i - n_t \cos\theta_t)}{(n_i \cos\theta_i + n_t \cos\theta_t)} \tag{5}$$

$$r_\parallel = \frac{(n_t \cos\theta_i - n_i \cos\theta_t)}{(n_t \cos\theta_i + n_i \cos\theta_t)}, \tag{6}$$

see Fig. 2. Note that the Fresnel reflection coeffecient is governed by the factors n_i, the refractive index of the surrounding medium, and n_t, the refractive index of the material. Both factors will be crucial for examining the effects that we measured. Due to energy conservation, the transmitted light is the light that is not being reflected off the surface and thus the Fresnel transmission coefficient is $F_t = 1 - F_r$.

Physics-Based BRDF Models assume that Fresnel reflection is the only process that is influenced by refractive index changes of the surrounding medium [TS67, CT81, HTSG91, APS00, MWAM05].

We show that current physics-based BRDF models do not adequately represent the refractive index dependence of the reflectance observed in reality. According to specular micro-facet BRDF models, the Fresnel effect is the dominant source of change in the shape of the reflectance lobes. For essentially diffuse objects, the Oren-Nayar [ON94] model predicts a constant BRDF.

We analyze the dependence of material reflectance properties on the refractive index of the surrounding medium. We present a measurement apparatus to measure isotropic refractive index-dependent bidirectional scattering distribution functions. We record a database of representative materials to verify the reflectance properties under refractive index changes.

Furthermore, we propose a method to measure the refractive index dependent BSDF and simultaneously determine the refractive index of the material sample.

4 BRDF Measurements

4.1 Measurement Setup

For the purpose of our experiment, we developed a new measurement setup. This setup allows to measure the BRDF of submerged materials. To our knowledge, existing devices are not suitable for acquiring reflectance data for samples immersed in a refractive medium.

Our setup is shown in Fig. 4. The material sample is immersed in a medium with a refractive index different from air. The cylinder contains the medium and the sample. A laser, mounted on a rotation stage, illuminates the sample from different angles. The laser ray hits the cylinder wall orthogonally for all acquisition angles, eliminating refraction upon entry into the medium, which would occur otherwise. A screen is attached directly to the cylinder wall in order to minimize the refraction on the exitant light path. The screen is imaged by a CCD camera (not shown), recording a slice of the sample BRDF attenuated by the BTDF of the screen.

To calibrate our system, we first compute the geometry of the setup using fiducial markers attached to the cylinder [SSS06]. We then proceed to calibrate the BTDF of the screen by recording a *calibration sample*. We use Labsphere Spectralon for this purpose [VZ06]. This material exhibits almost perfect Lambertian reflectance and a high albedo of $\approx 99\%$ for a wide range of wavelengths including the visible spectrum. To acquire the BTDF of the measurement screen we perform an image-based measurement that is valid for the geometric calibration determined previously.

First, we discuss the image formation in our BSDF measurement device. We refer to Fig. 3 for a description of the symbols used in the following. The radiance reflected from the sample is given by

θ_i^r, θ_o^r	incoming and outgoing angle w.r.t. normal for reflection at sample
θ_i^t, θ_o^t	incoming and outgoing angle w.r.t. normal for transmission at screen
ω_i^r, ω_o^r	incoming and outgoing angle for reflection at sample
ω_i^t, ω_o^t	incoming and outgoing angle for transmission at screen
f_r	BRDF of sample
f_t	BTDF of screen
$\Delta\omega_i^r$	solid angle subtended by laser as seen from sample
$\Delta\omega_i^t$	solid angle subtended by laser spot on sample as seen from screen
L_i^r	radiance incident on sample (from laser)
$L_o^r = L_i^t$	radiance exitant from sample (and incident on screen)
$L_o^t = L_c$	radiance exitant from screen (and recorded by camera)

(a) Table of symbols

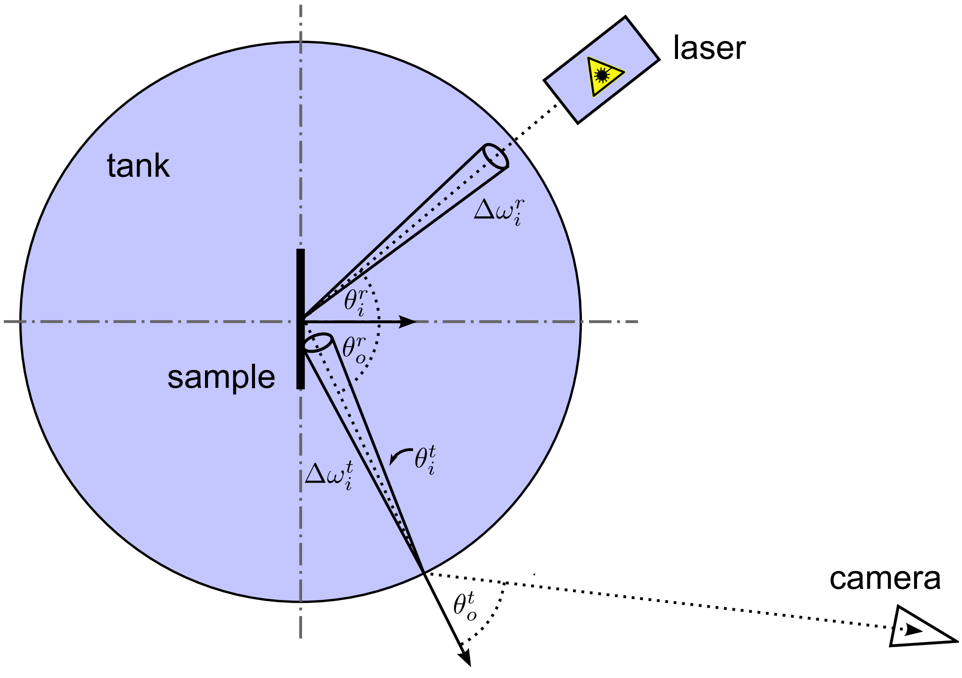

(b) BTDF calibration

Figure 3: The table of symbols used in the paper and the geometric layout for BTDF calibration

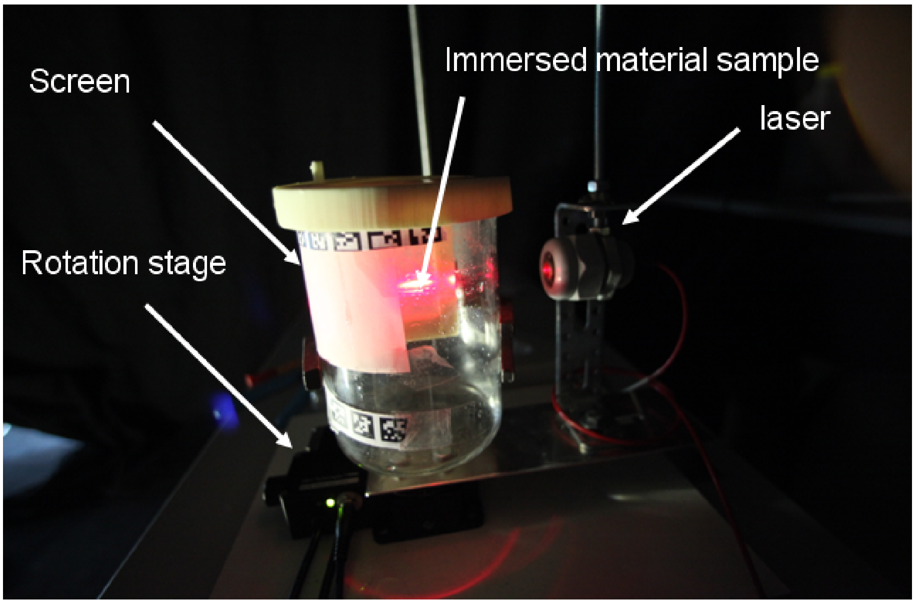

Figure 4: Our measurement setup: a material patch is placed in the diameter of the cylinder. The cylinder is filled with the surrounding medium. A rotating laser then shines in the range of 0° to 90°. The reflected light is imaged by a screen, which is attached to the cylinder and captured by a CCD camera.

$$L_o^r(\omega_o^r) = L_i^r(\omega_i^r) f_r(\omega_i^r, \omega_o^r) \cos\theta_i^r \Delta\omega_i^r. \quad (7)$$

We assume that L_i^r is approximately constant as opposed to Gaussian over $\Delta\omega_i^r$, therefore the integration is reduced to a simple multiplication. We will see that this assumption does not affect our calibration procedure. Similarly, the radiance registered by the camera is

$$L_c = L_o^t(\omega_o^t) = L_i^t(\omega_i^t) f_t(\omega_i^t, \omega_o^t) \cos\theta_i^t \Delta\omega_i^t, \quad (8)$$

and, as in the previous case, we assume $L_i^t(\omega_i^t)$ to be constant over $\Delta\omega_i^t$. This is only an approximation since the laser spot usually exhibits a Gaussian profile. Note, that $\Delta\omega_i^r$ varies as with $\cos\omega_i$ due to projected area foreshortening. Setting $\Delta\omega_i^t = \cos\theta_o^r \cdot c_0$, the cosine times some constant c_0 and combining Eqs. 7 and 8, we obtain

$$L_c = L_i^r(\omega_i^r) f_t(\omega_i^t, \omega_o^t) f_r(\omega_i^r, \omega_o^r) \cos\theta_i^t \cos\theta_o^t \cos\theta_i^r c_0. \quad (9)$$

This equation describes the recorded radiance due to a sample illuminated by a laser from direction ω_i^r.

Now, we perform a measurement with the *calibration sample*. We thus obtain a reference measurement

$$L_c^{Spectralon} = L_i^r(\omega_i^r) f_t(\omega_i^t, \omega_o^t) \frac{1}{\rho} \cos\theta_i^t \cos\theta_o^t \cos\theta_i^r c_0, \quad (10)$$

where $\frac{1}{\rho} \approx 0.99 \cdot \frac{1}{4\pi}$ is the BRDF of Spectralon. Now, taking an arbitrary BRDF measurement, Eq. 9, and dividing by the Spectralon reference measurement, Eq. 10, the geometric terms cancel and we obtain

$$f_r = \rho \cdot \frac{L_c}{L_c^{Spectralon}}, \quad (11)$$

i.e. we can directly measure a value proportional to the BRDF of the sample. Since we are recording a full slice of the BRDF for every incident angle of the laser, we perform the calibration for every laser angle. This is not strictly necessary since the diffuse BRDF of Spectralon does not vary with the incident angle. However, since our laser beam is only approximately centered we ensure a proper measurement this way.

Preprocessing

Each incident angle is imaged with different exposure times ($\frac{1}{4000}s$, $\frac{1}{1000}s$, $\frac{1}{250}s$, $\frac{1}{60}s$, $\frac{1}{25}s$, $\frac{1}{4}s$, $1s$) to account for the dynamic range of the reflected laser light. The resulting images for each incident angle are backprojected[Eve01] onto the surface of a cylinder which is fitted with RANSAC to the reconstructed geometry of the setup. Then, the backprojected images are combined to one HDR-image [MKMS07] which is then downsampled to size 249×180 px and stored according to the corresponding incident angle.

5 The ri-BRDF Model

We generalize the BRDF model for microfacet distributions to account for the refractive index in bidirectional scattering distribution functions. The refractive index of the surrounding medium n_i contributes to the Fresnel term for non-diffuse surface appearances. Thus, we model our refractive index dependent-BRDF (ri-BRDF) as

$$f_r(\omega_i, \omega_o, n_i, n_t) = \rho_d + \rho_s \cdot \frac{F_r(n_i, n_t) \cdot D(\omega_i, \omega_o) \cdot G(\omega_i, \omega_o)}{(4 \cdot \omega_i \cdot \omega_o)}, \tag{12}$$

where $D(\omega_i, \omega_o)$ is the microfacet distribution, e.g. a Blinn distribution, and $G(\omega_i, \omega_o)$ is the geometric attenuation term. The refractive index of the surrounding medium n_i is evaluated with the index of the material n_t in the Fresnel term $F_r(n_i, n_t)$ and modulates the appearance of the lobe. This refractive index dependent bidirectional scattering distribution model is a general way to represent materials with a given material index n_t that change the reflective and transmissive behavior according to the Fresnel equation. The parameter ρ_d accounts for the diffusely scattered light, while ρ_s modulates the intensity of the specular highlight. Typically, the angular extent of the highlight is modulated by an exponential parameter in the microfacet distribution D.

We evaluate the proposed BRDF model with the captured data for each acquired material. The fitting is based on the Levenberg-Marquard non-linear optimization [MNT04] and optimizes the parameters ρ_d,ρ_s,n_t and the exponent of the microfacet distribution. We chose a Blinn microfacet distribution. Since it is crucial for the fitting process to find a good initial guess, we calculate the mean intensity of the diffusely scattered light for each measured refractive index and assign it to ρ_d. The parameter ρ_s is initially assigned the mean intensity value of the reflected light, i.e. $\omega_o = \omega_i$, for each measured refractive index. The index of the material is assigned to n_t. For the initial damping parameter we employ $\tau = 0.1$ and for the convergence criterion $\epsilon_1 = \epsilon_2 = 10^{-6}$, as proposed by Madsen et al. [MNT04]. The fitting usually converges after about 20 iterations. A typical fitting result for materials showing the behaviour governed by the Fresnel term is shown in Fig. 6.

Material	ρ_d	ρ_s	n_t	exp	k
Bamboo	0.164	0.399	1.292	20.061	48
Cloth	0.871	2.782	1.356	9.849	9
Plastic	1.5853	0.407	1.323	299.536	8
Sandpaper	0.200	6.851	0.596	4.732	19
Ceramics	0.558	4.269	1.300	20.276	49

Table 1: The fitting results for the proposed model with different materials that show the reflectance behavior governed by the Fresnel term. The table lists the model parameters ρ_d, ρ_s, the estimated refractive index of the material n_t, the exponent for the microfacet distribution, and the number of iterations k needed for the fitting process to converge.

6 Results

In the first step we fitted the proposed BRDF model to the captured BRDF data in our database. We captured the following classes of materials: Acrylic paint, aluminum, bamboo, ceramics, cloth, oil paint, plastic, sandpaper, stone, Teflon and wood. We found that only bamboo, cloth, ceramics plastic and sandpaper show significantly different reflectance behaviour for different media. The other materials did not show a different reflectance behaviour for different refractive indices, Fig. 5. Table 1 shows the results for the fitting of the proposed model to the captured BRDF data of materials that show the reflectance behaviour governed by the Fresnel term. We implemented the proposed BRDF model in the physics-based renderer PBRT [PH04] to enable rendering of objects in media with different refractive indices. To render our results, Fig. 1 and in the accompanying video, we loaded the measured BRDF-data in the MERL-file format[MPBM03b]. The scenes are assembled using Cinema 4D and Realflow fluid simulation. The parts of the obstacle that are hit by the fluid are assigned the BRDF of distilled water, while the remaining parts are assigned the BRDF of air. The light-water interaction was computed using a photon mapping integrator. The rendering time took approximately 10 minutes per frame on a 2.2 Ghz Intel Core 2Duo processor with a NVIDIA GeForce G210M graphics card, the image resolution was 768×576 pixel. In a second step we synthesized the BRDFs of air and salt solutions with our proposed BRDF model, the parameters were determined by fitting the model to the measured BRDF-data, Fig. 7.

We state that the proposed BRDF model is only applicable for materials that show behaviour governed by the Fresnel term. Moreover, the presented BRDF model is only isotropic. It does not model retroreflective effects due to the fact that we only sample one of the two angles for the incident direction and that we sample only half the hemisphere with the screen.

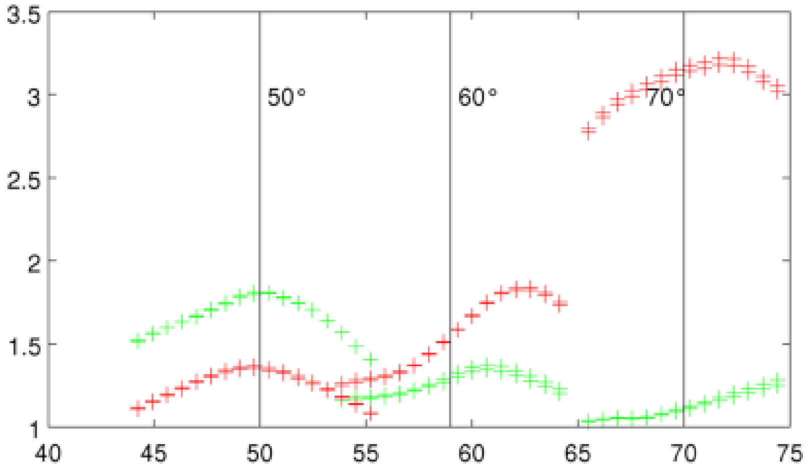

Figure 5: Aluminum is one of the materials that does **not** show the predicted behavior. The plot shows the measured reflectance data (dots) for incident angles 50°,60° and 70° w.r.t. the surface normal for refractive indices 1.0 (red) and 1.44 (green). The exitant reflectance are measured for $\phi_o = 0°$ and $\theta_o \in [45°, 75°]$. Note, that the reflectances vary only in a small numeric range.

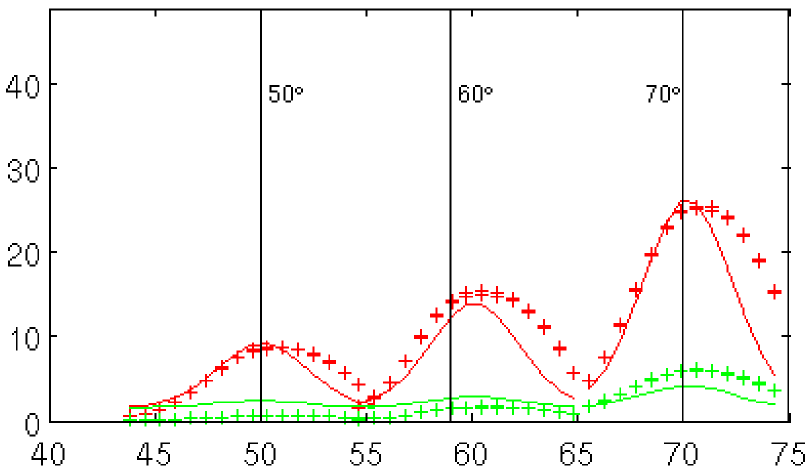

Figure 6: The fitting results for red plastic. The plot shows the measured reflectance data (dots) for incident angles 50°,60° and 70° w.r.t. the surface normal and the fitting of the proposed model (lines) for refractive indices 1.0 (red) and 1.44 (green). The exitant reflectances a measured for $\phi_o = 0°$ and $\theta_o \in [45°, 75°]$. The vertical lines denote $\theta_o = \theta_i$ for each incident angle. Note the underestimation of values with increasing incident angle.

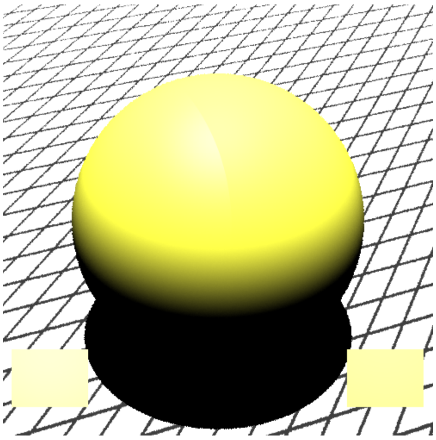

(a) Bamboo (fitted)

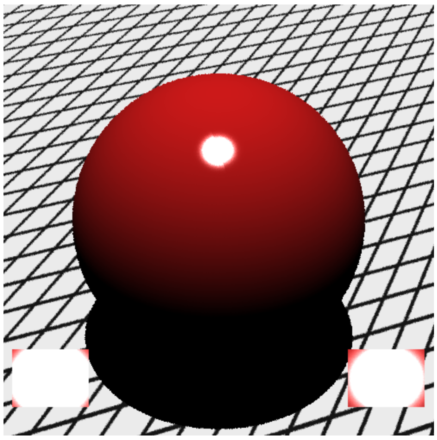

(b) Plastic (fitted)

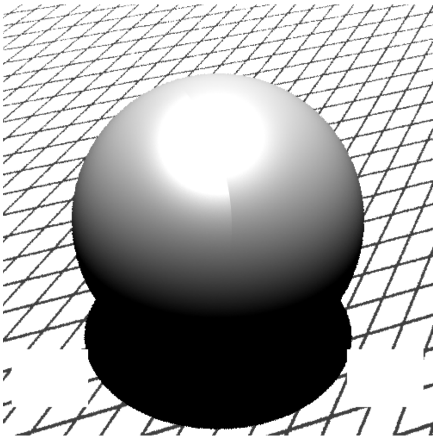

(c) Ceramics (fitted)

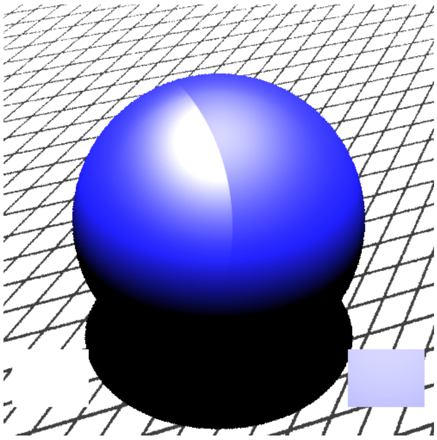

(d) Cloth (fitted)

Figure 7: The effects of different surrounding media to the size of the specular reflection in the proposed model: In each image, the left side of the sphere shows the reflection of the material for air (≈ 1.0) and the right side shows for a medium with refractive index ≈ 1.2. The small boxes show a close-up view to the particular highlight. Note, that the intensity (a,b,c,d) and the extend of the highlight (a,c,d) decreases with increasing refractive index

7 Conclusion

We have investigated the effect of immersing a material into different media and compared the measured behavior with the prediction of the Fresnel term. We presented a new method to measure the material behaviour by placing it at the center of a cylinder and imaging the reflected laser light with a screen attached to the cylinder. The measured data were preprocessed and fitted with the proposed microfacet-based BRDF-model that considers the refractive index of the surrounding medium as a variable for the Fresnel term. We validated our model by implementing it in a physics-based renderer. In the future we want to extend the measurement setup to account for anisotropic materials and retroreflectance. Furthermore we want to investigate the effect with submerged multi-layer materials.

Acknowledgements

References

[APS00] Michael Ashikmin, Simon Premože, and Peter Shirley. A Micro-Facet Based BRDF Generator. In *Proc. of SIGGRAPH*, pages 65–74, 2000.

[Bli77] James F. Blinn. Models of Light Reflection for Computer Synthesized Pictures. In *Proc. of SIGGRAPH*, pages 192–198, 1977.

[Bra03] Mathew Brand. Charting a Manifold. *NIPS*, 15:985–992, 2003.

[BS63] Petr Beckmann and André Spizzichino. *The Scattering of Electromagnetic Waves from Rough Surfaces.* Pergamon Press, 1963.

[CT81] Robert L. Cook and Kenneth E. Torrance. A Reflectance Model for Computer Graphics. In *Proc. of SIGGRAPH*, pages 307–316, 1981.

[Dan01] Kristin J. Dana. BRDF/BTF Measurement Device. In *Proc. of ICCV*, pages 265–272, 2001.

[DWL+09] Qiang Dai, Jiaping Wang, Yiming Liu, John Snyder, Enhua Wu, and Baining Guo. The Dual-microfacet Model for Capturing Thin Transparent Slabs. *CGF*, 28(7):1917–1925, 2009.

[Eve01] C. Everitt. Projective texture mapping. *White paper, NVidia Corporation*, 2001.

[GHAO08] Abhijeet Ghosh, Wolfgang Heidrich, Shruthi Achutha, and Matthew O'Toole. A Basis Illumination Approach to BRDF Measurement. *IJCV*, 2008.

[GRBN07] Jinwei Gu, Ravi Ramamoorthi, Peter Belhumeur, and Shree K. Nayar. Dirty Glass: Rendering Contamination on Transparent Surfaces. In *Proc. of EGSR*, pages 159–170, 2007.

[HHA+10] Matthias B. Hullin, Johannes Hanika, Boris Ajdin, Jan Kautz, Hans-Peter Seidel, and Hendrik P. A. Lensch. Acquisition and Analysis of Bispectral BRDFs. *Trans. Graph.*, 29(3):to appear, 2010.

[HK93] Pat Hanrahan and Wolfgang Krueger. Reflection from Layered Surfaces due to Subsurface Scattering. In *Proc. of SIGGRAPH*, pages 164–174, 1993.

[HTSG91] Xiao D. He, Kenneth E. Torrance, François X. Sillion, and Donald P. Greenberg. A Comprehensive Physical Model for Light Reflection. In *Proc. of SIGGRAPH*, pages 175–186, 1991.

[JMLH01] H.W. Jensen, S.R. Marschner, M. Levoy, and P. Hanrahan. A practical model for subsurface light transport. In *Proceedings of the 28th annual conference on Computer graphics and interactive techniques*, pages 511–518. ACM, 2001.

[Kaj85] James T. Kajiya. Anisotropic Reflection Models. In *Proc. of SIGGRAPH*, pages 15–21, 1985.

[KM99] J. Kautz and M.D. McCool. Interactive rendering with arbitrary BRDFs using separable approximations. In *Eurographics Rendering Workshop 1999*, volume 18. Citeseer, 1999.

[KSK01] C. Kelemen and Laszlo Szirmay-Kalos. A Microfacet-Based Coupled Specular-Matte BRDF Model with Importance Sampling. In *Proc. of Eurographics (Short Papers)*, pages 25–34, 2001.

[LFTG97] Eric P. F. Lafortune, Sing-Choong Foo, Kenneth E. Torrance, and Donald P. Greenberg. Non-linear Approximation of Reflectance Functions. In *Proc. of SIGGRAPH*, pages 117–126, 1997.

[LGR+05] Jianye Lu, Athinodoros S. Georghiades, Holly Rushmeier, Julie Dorsey, and Chen Xu. Synthesis of Material Drying History: Phenomenon Modeling, Transferring and Rendering . In *Proc. of Workshop on Natural Phenomena*, pages 175–184, 2005.

[LKG+03] Hendrik P. A. Lensch, Jan Kautz, Michael Goesele, Wolfgang Heidrich, and Hans-Peter Seidel. Image-based Reconstruction of Spatial Appearance and Geometric Detail. *Transactions on Graphics*, 22(2):234–257, 2003.

[MKMS07] Rafał Mantiuk, Grzegorz Krawczyk, Radosław Mantiuk, and Hans-Peter Seidel. High dynamic range imaging pipeline: Perception-motivated representation of visual content. In Bernice E. Rogowitz, Thrasyvoulos N. Pappas, and Scott J. Daly, editors, *Human Vision and Electronic Imaging XII*, volume 6492 of *Proceedings of SPIE*, San Jose, USA, February 2007. SPIE.

[MMS+05] Gero Müller, Jan Meseth, Mirko Sattler, Ralf Sarlette, and Reinhard Klein. Acquisition, Synthesis and Rendering of Bidirectional Texture Functions. *CGF*, 24(1):83–109, 2005.

[MNT04] K. Madsen, H.B. Nielsen, and O. Tingleff. Methods for non-linear least squares problems. *Technical University of Denmark*, 2:4, 2004.

[MPBM03a] Wojciech Matusik, Hanspeter Pfister, Matt Brand, and Leonard McMillan. A Data-Driven Reflectance Model. *Transactions on Graphics*, 22(3):759–769, 2003.

[MPBM03b] Wojciech Matusik, Hanspeter Pfister, Matt Brand, and Leonard McMillan. A data-driven reflectance model. *ACM Transactions on Graphics*, 22(3):759–769, July 2003.

[MPBM03c] Wojciech Matusik, Hanspeter Pfister, Matt Brand, and Leonard McMillan. Efficient Isotropic BRDF Measurement. In *Proc. of EGSR*, pages 241–247, 2003.

[MWAM05] Stephen R. Marschner, Stephen H. Westin, Adam Arbree, and Jonathan T. Moon. Measuring and Modeling the Appearance of Finished Wood. *Trans. Graph.*, 24(3):727–734, 2005.

[MWLT00] Stephen R. Marschner, Stephen H. Westin, Eric P. F. Lafortune, and Kenneth E. Torrance. Image-based Bidirectional Reflectance Distribution Function Measurement. *Applied Optics*, 39(16):460–466, 2000.

[NDM05] Addy Ngan, Fredo Durand, and Wojciech Matusik. Experimental Analysis of BRDF Models. In *Proc. of EGSR*, pages 117–126, 2005.

[ON94] Michael Oren and Shree K. Nayar. Generalization of Lambert's Reflectance Model. In *Proc. of SIGGRAPH*, pages 239–246, 1994.

[PF90] Pierre Poulin and Alain Fournier. A Model for Anisotropic Reflection. In *Proc. of SIGGRAPH*, pages 273–282, 1990.

[PH04] M. Pharr and G. Humphreys. *Physically based rendering: From theory to implementation*. Morgan Kaufmann, 2004.

[Pho75] Bui Tuong Phong. Illumination for Computer Generated Pictures. *Comm. ACM*, 18(6):311–317, 1975.

[Sch94] Christophe Schlick. An Inexpensive BRDF Model for Physically-Based Rendering. *Computer Graphics Forum*, 13(3):233–246, 1994.

[SSR+07] Bo Sun, Kalyan Sunkavalli, Ravi Ramamoorthi, Peter N. Belhumeur, and Shree K. Nayar. Time-Varying BRDFs. *TVCG*, 13(3):595–609, 2007.

[SSS06] N. Snavely, S. Seitz, and R. Szeliski. Photo Tourism: Exploring image collections in 3D. *ACM Transactions on Graphics (Proceedings of SIGGRAPH 2006)*, 2006.

[TS67] K. E. Torrance and E. M. Sparrow. Theory for Off-Specular Reflection from Roughened Surfaces. *JOSA*, 57(9):1105–1114, 1967.

[VZ06] Kenneth J. Voss and Hao Zhang. Bidirectional Reflectance of Dry and Submerged Labsphere Spectralon Plaque. *Applied Optics*, 45(30):7924–7927, 2006.

[War92] G. J. Ward. Measuring and Modeling Anisotropic Reflection. In *Proc. of SIGGRAPH*, pages 265–272, 1992.

[WMLT07] Bruce Walter, Stephen R. Marschner, Honsong Li, and Kenneth E. Torrance. Microfacet Models for Refraction through Rough Surfaces . In *Proc. of EGSR*, pages 195–206, 2007.

[WMLT08] B. Walter, S.R. Marschner, H. Li, and K.E. Torrance. Eurographics Symposium on Rendering (2007) Jan Kautz and Sumanta Pattanaik (Editors) Microfacet Models for Refraction through Rough Surfaces. 2008.

[WW07] Andrea Weidlich and Alexander Wilkie. Arbitrarily Layered Micro-Facet Surfaces. In *Proc. of Pacific Graphics*, pages 171–178, 2007.